Anal Bioanal Chem (2017) 409:1519–1529
DOI 10.1007/s00216-016-0088-6

RESEARCH PAPER

Visible and red emissive molecular beacons for optical temperature measurements and quality control in diagnostic assays utilizing temperature-dependent amplification reactions

Zerrin Fidan[1] · **Andy Wende**[2] · **Ute Resch-Genger**[1]

Received: 24 August 2016 / Revised: 31 October 2016 / Accepted: 7 November 2016 / Published online: 29 November 2016

Abstract Quality control requirements imposed on assays used in clinical diagnostics and point-of-care-diagnostic testing (POCT), utilizing amplification reactions performed at elevated temperatures of 35 to 95 °C are very stringent. As the temperature of a reaction vessel has a large impact on the specificity and sensitivity of the amplification reaction, simple tools for local in situ temperature sensing and monitoring are required for reaction and assay control. We describe here a platform of stem-and-loop structured DNA hairpins (molecular beacons, MBs), absorbing and emitting in the visible and red spectral region, rationally designed for precise temperature measurements in microfluidic assays for POCT, and their application for temperature measurements in a common DNA-based molecular biological assay utilizing thermophilic helicase-dependent amplification (tHDA). Spectroscopic studies of these MBs, rationally designed from DNA sequences of different thermal stabilities, chosen not to interact with the DNA probes applied in the nucleic acid amplification assay, and temperature-dependent fluorescence measurements of MB-assay mixtures revealed the suitability of these MBs for temperature measurements directly in such an assay with a temperature resolution of about 0.5 °C without interferences from assay components. Combining two spectrally distinguishable MBs provides a broader response range and an increase in temperature sensitivity up to 0.1 °C. This approach will find future application for temperature monitoring and quality control in commercialized diagnostics assays using dried reagents and microfluidic chips as well as assays read out with tube and microplate readers and PCR detection systems for temperature measurements in the range of 35 to 95 °C.

Keywords Fluorescence molecular beacon · Temperature sensing · Microfluidics · Quality assurance · Diagnostic assay · DNA amplification

Introduction

Temperature is a key parameter for chemical reactions and biochemical processes such as enzymatic reactions, protein folding, and molecular interactions. Also, it largely affects the mechanical, optical, and structural properties of biomolecules like proteins and DNA [1]. Hence, local and precise temperature measurements at micro- and nanoscales are crucial for cellular biology, medical diagnostics, biotechnology, and process control. Moreover, there is an increasing need for in situ temperature sensing and constant temperature monitoring in molecular biological assays utilizing amplification reactions performed at elevated temperatures between 35 and 95 °C to meet the stringent requirements on quality control imposed on assays used in clinical diagnostics and point-of-care-diagnostic testing (POCT) [2]. This is related to the fact that the specificity and sensitivity of sequence-specific nucleic acid amplification reactions depend on accurate reaction conditions, e.g., buffer composition, magnesium concentration, and temperature settings. Therefore, molecular diagnostic tests must always include internal controls

Electronic supplementary material The online version of this article (doi:10.1007/s00216-016-0088-6) contains supplementary material, which is available to authorized users.

✉ Ute Resch-Genger
ute.resch@bam.de

[1] Federal Institute for Materials Research and Testing (BAM), Richard-Willstaetter-Str. 11, 12489 Berlin, Germany

[2] QIAGEN GmbH, Qiagen Straße 1, 40724 Hilden, Germany

to prove that the amplification reaction was not compromised by wrong settings or the presence of inhibitory substances [3]. For assays relying on isothermal amplification technologies such as loop-mediated isothermal amplification (LAMP)[4] or thermophilic helicase-dependent amplification (tHDA) [5, 6], but also for conventional polymerase chain reaction (PCR) [7, 8], this implies particularly the signaling (yes/no answer) that a certain temperature has been reached.

Optical temperature sensors are particularly attractive for non-invasive and non-contact temperature measurements in cells or in rotating microfluidic systems, which have emerged as a powerful tool for medical diagnostic applications and POCT solutions. These sensors bypass some of the limitations of other technologies. This includes, e.g., invasiveness in the case of thermocouples and electrical sensors requiring contact and the lack of spatial resolution of noncontact methods such as IR thermography [1, 9]. Features of an ideal non-invasive fluorescent temperature sensor include a high fluorescence intensity for sensitive temperature measurements to overcome interferences from, e.g., background emission from biological compounds, a fast response time, a high chemical stability under application-relevant conditions, and a high reversibility. Favorable are also the simple tuning of the temperature sensing range as prerequisite for versatile applications and the suitability for multiplexing, e.g., a multicolor approach. Moreover, applications in diagnostics assays and POCT [2] can require temperature measurements in a cocktail of different compounds and, hence, the prevention of interferences with other assay components.

Luminescent temperature sensors have been prepared from different classes of molecular luminophores and fluorescent nanoparticles and typically utilize temperature-dependent fluorometric parameters like luminescence intensity (or intensity ratios) and lifetime as well as spectral band position and width [1, 9–11]. Examples include temperature-sensitive organic dyes [12–17], luminescent metal-ligand complexes like lanthanide-based molecular thermometers [10, 18, 19], fluorophores embedded into or bound to particles [20–23] or attached to polymers [24, 25], polymer-based nanogels [26, 27], and fluorescent gold nanoparticles [28]. Frequently, combinations of temperature-sensitive and temperature-insensitive dyes, that can be excited at the same wavelength, but reveal spectrally distinguishable emission bands, are used for referenced or ratiometric dual color (e.g., dual-emission-wavelength) temperature measurements. This renders temperature measurements independent of fluctuations in the excitation light intensity, sensor concentration and, hence, photobleaching, and optical path length [10]. This can be also realized with dual or multicolor emissive materials like up-converting phosphors [29–31] or time-resolved fluorescence methods can be employed [10, 18, 32].

A particularly attractive approach for non-invasive fluorescence-based temperature sensing are small size stem-and-loop structured DNA hairpins or molecular beacons (MBs) [33] that reveal unique temperature-dependent structural features [18, 34–38]. These biocompatible, flexible single-stranded oligonucleotides can be dually labeled at their 5′ and 3′ ends with a fluorophore and a quencher or with two spectrally distinguishable fluorophores. Typically, a fluorescent organic dye or occasionally a lanthanide chelate is combined with an absorbing and non-emissive acceptor like an organic azo dye or increasingly, a gold or silver particle with a strong surface plasmon resonance absorption or a carbon nanotube or, for ratiometric temperature measurements, with another fluorophore. The fluorescence properties of such MBs are controlled by the conformation of the stem region, which defines the distance between the labels attached to both ends of the MB and, hence, by temperature, exploiting distance-dependent interaction and quenching mechanisms like fluorescence resonance energy transfer (FRET) or less frequently, electron transfer [18, 33, 35, 39–41]. MBs bearing fluorophore-quencher pairs are emissive in the open form and non-fluorescent in the closed form. Dual fluorophore-labeled MBs display emission from the acceptor fluorophore upon donor excitation in the closed form, whereas the larger distance between donor and acceptor fluorophores open random-coil conformation prevents FRET [37].

For temperature monitoring and quality control in diagnostics assays with a resolution better than 1 °C (0.5 to 0.1 °C desired), we developed a platform of MBs with emission in the visible (vis) and red (emission >650 nm), which can be directly integrated into different types of DNA-based assays run on various platforms including microfluidic chips and rotating disks [42]. Particularly in the latter case, precise temperature measurements in the assay cocktail are restricted to optical measurements as other common and simple methods like the use of thermocouples and electrical sensors are hampered by the rotation. For eventual application in routine molecular diagnostics, also a simple integrating step of the optical temperature sensor like the use of freeze-dried components as used for some commercial DNA-based assays seemed favorable. In this proof-of-concept study, we address challenges like the choice of suitable fluorescent reporters, which can be read out in different detection channels than the assay-specific DNA probes, and possible cross hybridization with DNA sequences of the actual assay. Both are essential factors to consider since it is desired to perform the MB-based temperature measurement in the same reaction vessel as the actual diagnostic assay. In the following, the design criteria for such MBs are presented including spectroscopic studies of representative MBs in typical assay buffers and typical MB-assay mixtures with special emphasis on tHDA. As a proof-of-

concept experiment, a first tHDA assay was performed with the MBs located in the assay reaction mixture containing the enzymes, and the analyte-specific primer/probe set, here a *Mycobacterium tuberculosis* IS6110 probe/primer set and *M. tuberculosis* genomic DNA.

Experimental

Materials

ATTO 647N was purchased from ATTO-Tec, ROX (6-carboxy-X-rhodamine) from BioSearch Technologies (CA, USA), quenchers 661Q and Q3 from Dyomics, BHQ-2 and BHQ-3 from Biosearch, respectively. Bovine serum albumin (BSA) was obtained from Merck KGaA (BSA, fraction V) and all MBs from Eurogentec. For the spectroscopic studies of the dyes, quenchers, and MBs, we used phosphate-buffered saline (PBS) (137 mM NaCl, 2.7 mM KCl, 10 mM Na2HPO4, 1.8 mM KH2PO4, pH 7.4) and HDA buffer (proprietary mixture). The dyes and quenchers were additionally assessed in PBS containing 10 mass-% of BSA (PBS/BSA) for quencher choice. The chemical structures of dyes and quenchers used for MB design are provided in the Electronic Supplementary Material (ESM; Fig. S1) and the sequences of all MBs are given in the section on MB design.

Instrumentation

Absorption spectra were recorded on a calibrated Cary 5000 spectrometer (Varian), which was equipped with a thermostat (temperature regime: about −10 to 95 °C) for temperature-dependent measurements of absorption spectra. Fluorescence measurements were performed with a calibrated Edinburgh Instruments FSP 920 spectrofluorometer [43]. For temperature-dependent fluorescence measurements, a thermostat (temperature regime from −10 to 95 °C) was used. Prior to its use, the thermostat was calibrated with an external temperature sensing device or probe which was calibrated with an accuracy of ±0.1 °C. This external temperature probe was always used to control the reliability of our temperature-dependent spectroscopic measurements. Absolute measurements of the fluorescence quantum yields (Φ_f) of the free labels ROX and ATTO 647N in PBS and in HDA buffer were done at room temperature ($T = (25 \pm 1)$ °C) in duplicate at two different concentrations (absorbance at the excitation wavelength <0.1) with the calibrated stand-alone integrating sphere setup Quantaurus C11347-11 from Hamamatsu Photonics and corrected for reabsorption using the previously assessed reabsorption correction from the instrument manufacturer [44]. HDA experiments were done with the real-time PCR instrument Rotor-Gene Q (QIAGEN, Germany), which features up to six separated channels for fluorescence acquisition and precise temperature control.

Calculation of MB sequences

For the choice of suitable MB sequences, the two-dimensional structure of single-strand oligonucleotides and particularly the melting temperature T_m of the resulting double-stranded stem structures were calculated using the software OligoAnalyzer 3.1 (http://eu.idtdna.com/calc/analyzer), which is based on UNAFold algorithms [45].

Measurement conditions

All absorption and fluorescence measurements were performed with air-saturated freshly prepared dye and MB solutions at $T = (25 \pm 1)$ °C using 10 mm × 10 mm quartz cuvettes from Hellma GmbH and excitation wavelengths of 550 and 600 nm for ROX and ATTO 647N, respectively. For measurements with the integrating sphere setup, 10 mm × 10 mm long-necked quartz cuvettes from Hamamatsu Photonics K.K. were employed, always filled with 3.5 ml of solvent or dye solution [44]. Typically, a dye (or species) concentration of 2×10^{-6} mol/l was used and a MB concentration of 1×10^{-3} mol/l, respectively. All emission spectra reported present spectrally corrected spectra referenced to the spectral photon radiance scale [46]. The uncertainties of the absolutely measured Φ_f of ROX and ATTO 647N including instrument calibration and all corrections are estimated to be ±6% as derived from previous measurements in this wavelength region [43, 44].

The temperature dependence of Φ_f of ROX and ATTO 647N was obtained from temperature-dependent absorption factors and integral fluorescence intensities derived from the corresponding absorption and spectrally corrected emission spectra (integration over the complete emission band on a photonic scale) [46] using absolutely measured Φ_f at $T = (25 \pm 1)$ °C as reference [43]. The Förster radii R_0 of the FRET pairs ROX-BHQ2 and ATTO 647N-BHQ3 were calculated from the measured spectroscopic data of the donors and acceptors assuming κ of 2/3 [47] and using the molar absorption coefficients of 38,000 and 42,700/M/cm, respectively, as provided by Biosearch. The melting curves of all single MBs and MB mixtures and T_m values were obtained by plotting the fluorescence intensity measured at the dye's emission maximum against the temperature in the temperature range of 20 to 85 or 90 °C. The fluorescence intensities were normalized to the value at the highest temperature, i.e., 85 or 90 °C, respectively. The uncertainties, i.e., relative standard deviations were

derived from at least three independent measurements. A representative example for achievable uncertainties is given in the ESM (see Fig. S7).

tHDA experiments

tHDA reactions were prepared by mixing the following components in 0.1 ml Rotor-Gene Q Strip Tubes (QIAGEN, Germany): 8 μl 2.5× reagent buffer, 2 μl *M. tuberculosis* IS6110 specific primer/probe set containing 100 nM MB (final concentration), 1 μl enzyme mix (UvrD-type helicase, DNA polymerase, single-strand binding protein), 2 μl 10× magnesium sulfate solution, 1 μl *M. tuberculosis* genomic DNA as template, and water to a final volume of 20 μl. The amplification probe was double-labeled, with the fluorophore being attached at the 5′ end and a quencher at the 3′ end of the oligonucleotide chain. The reaction mixture was placed in the real-time PCR instrument Rotor-Gene Q and incubated at 63 °C for 40 min in the Rotor-Gene Q for isothermal amplification of the DNA template. During the incubation, the fluorescence of ROX (orange channel) and Atto 647N (red channel) were measured in intervals of 1 min. When the isothermal amplification reaction was finished, melting curves of all amplification reactions were acquired using the same instrument by applying the following temperature profile: 1 min 95 °C initial melting step, cool down to 35 °C, stepwise (0.5 °C steps) temperature increase from 35 to 95 °C with acquisition of the fluorescence of ROX and Atto 647N, respectively. In order to guarantee temperature equilibration, fluorescence acquisition was preceded by a 5-s time interval. The reversibility of the melting curves and the absorption and fluorescence of the MBs was always controlled.

Results and discussion

Molecular beacon design—choice of fluorophores and quenchers

Crucial for the development of MB-based optical thermometers, which can be integrated as internal temperature control into a broad variety of DNA-based diagnostic assays, is the proper choice of suitable fluorophores, quenchers, and MB sequences. This implies covering the assay-specific temperature range and minimum temperature to be guaranteed, considering the optical properties of other fluorescent DNA probes present in the reaction mixture, and circumventing interferences with assay components. For sensitive temperature measurements, a complete or at least a very strong quenching of the fluorescence in the closed form of the MB and, hence, efficient FRET under application-relevant conditions, is desired and a strong emission in the open form. This requires a high Φ_f of the reporter dyes and a large spectral overlap between the emission band of the fluorescent donor and the absorption band of the non-emissive or emissive acceptor in typical assay buffers. Thus, the temperature dependence of the spectral position and intensity of the absorption and fluorescence bands of the fluorophores and non-emissive quenchers must be preferably very small. Otherwise, the signals at elevated temperatures are reduced and FRET efficiencies become temperature dependent. This limits especially the number of suitable fluorescent reporters to dyes with a rigid molecular structure, where all molecular rotations leading to a temperature-dependent radiationless deactivation of the excited singlet state are blocked. Classical examples include the vis emitter rhodamine 101 and its derivatives [22, 48, 49] and recently discovered coumarin 545 [50]. This is a particular challenge for long wavelength MBs, as fluorophores with a temperature-insensitive emission in the red spectral region are rather rare. Moreover, for fluorophore-quencher pairs, the quencher needs to be fluorometrically silent not only in aqueous or buffer solutions but also in the presence of common additives like proteins and surfactants.

As vis fluorophore for our temperature-sensing MBs, we chose the rhodamine ROX and as red fluorophore the carbopyronine ATTO 647N, which is increasingly applied as a substitute for the ozone sensitive cyanine Cy5 [51]. The rigid structure of the latter fluorophore suggests a small temperature dependence of its fluorescence properties. Moreover, ROX and Atto 647N are highly emissive and are known for their high thermal and photochemical stability. The absorption and emission spectra of both dyes in PBS are shown in Fig. 1 (left panels). Subsequently performed studies of the temperature dependence of the spectral features and Φ_f of both dyes, summarized in Table 1 and right panels of Fig. 1, reveal minimum spectral shifts in absorption and emission with increasing temperature and very high fluorescence quantum yields of 82.8 and 58.9%, which barely decrease at elevated temperatures. The spectroscopic features of ROX and ATTO 647N in HDA buffer used for our diagnostic assay, closely resemble those in PBS (ROX: $\lambda_{max,abs} = 580$ nm, $\lambda_{max,em} = 603$ nm, $\Phi_f = 77.0$; ATTO 647N: $\lambda_{max,abs} = 647$ nm, $\lambda_{max,em} = 668$ nm, $\Phi_f = 61.6$; 25 °C), see also ESM (Fig. S2).

As potential non-emissive quenchers, we evaluated the polyaromatic azo Black Hole quenchers BHQ2 and BHQ3 and the quenchers 661Q and Q3, which all revealed a strong spectral overlap with the emission of either our vis or red fluorescent label. In order to avoid signal contributions from the quencher and guarantee efficient FRET also at higher temperatures, the quencher should be fluorometrically silent at application-relevant conditions and reveal only a small temperature dependence of their absorption properties as prerequisite for efficient quenching of the reporter dyes also at higher temperatures. For use in molecular diagnostic assays, the former criterion implies complete fluorescence quenching in the

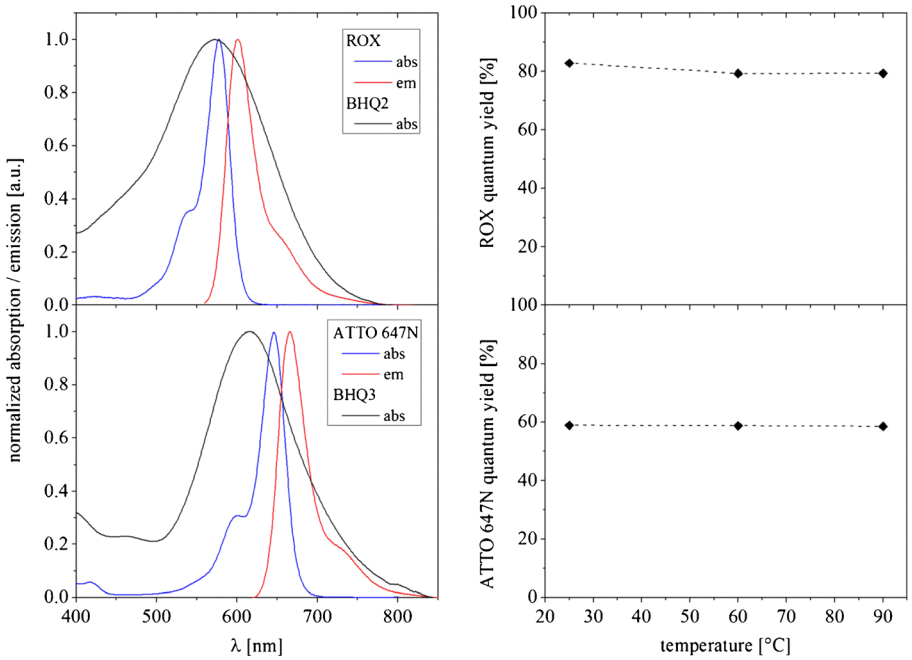

Fig. 1 *Left*: Normalized absorption and emission spectra of ROX and ATTO 647N and normalized absorption spectra of the quenchers BHQ2 and BHQ3 in PBS at $T = 25$ °C. *Right*: Temperature dependence of Φ_f of ROX and ATTO 647N in PBS (selected data points covering the temperature region of interest). The absorption and emission spectra of the dyes and quenchers in the buffer HDA used for the molecular diagnostic assays and temperature measurements of the molecular beacons in the assay mixture closely match with the corresponding spectra in PBS (see also Table 1)

presence of common assay additives like certain surfactants and proteins. Subsequent spectroscopic studies of the four quenchers in PBS and PBS/BSA revealed some fluorescence for 661Q and Q3 in PBS/BSA, whereas BHQ2 and BHQ3 remained non-emissive also in the presence of BSA. Moreover, BHQ2 and BHQ3 undergo only slight spectral shifts of their broad absorption bands with increasing temperature (see Fig. 1, left panels, and Table 1 and ESM, Fig. S4), with the size of this temperature-induced spectral shift being more pronounced for BHQ3 (see Table 1). The Förster radii R_0 for the FRET pairs ROX-BHQ2 and ATTO 647N-BHQ3, which represent a measure for FRET efficiency, were determined to 60.2 and 58.1 Å in PBS at 25 °C and to 60.2 and 62.8 Å at 90 °C, respectively (see also ESM, Fig. S3, and equations used for the calculation of R_0). For ROX-BHQ2 and ATTO 647N-BHQ3 in HDA buffer, R_0 amounted to 58.6 and 60.3 Å at 25 °C. This provides the basis for the desired efficient signal generation together with the high Φ_f of the chosen reporter dyes.

MB sequences

Crucial for the desired measurements of temperature directly in the assay mix and not in a separate chamber is the choice of a suitable MB sequence as this implies the prevention of a potential cross hybridization with DNA sequences from the actual assay under the respective assay conditions, i.e., the respective buffer and reaction temperature. Here, it needs to be considered that a MB molecule consists of two separate structural regions, a stem and a loop region. The stem region is formed by hybridization of the two complementary nucleotide sequences located at the 5′ and 3′ end of the same oligonucleotide molecule. These nucleotide sequences are connected by the loop region, which, by design must not be complementary

Table 1 Spectroscopic properties of ROX, ATTO 647N, BHQ2, and BHQ3 in PBS at 25 °C and at 90 °C and in HDA buffer at 25 °C, respectively

Sample	T [°C]	$\lambda_{abs,max}$ [nm] PBS	$\lambda_{em,max}$ [nm]	$\lambda_{abs,max}$ [nm] HDA	$\lambda_{em,max}$ [nm]
ROX	25	577	602	580	603
ATTO 647N	25	646	666	647	668
BHQ2	25	564	–	582	–
BHQ3	25	615	–	620	–
ROX	90	575	599	–	–
ATTO 647N	90	646	667	–	–
BHQ2	90	564	–	–	–
BHQ3	90	642	–	–	–

The corresponding absorption and emission spectra are shown in the ESM (Figs. S2–S4, S7 and S8 exemplarily for ROX and BHQ2 attached to a MB in HDA buffer)

to the stem regions and to other DNA molecules in the assay cocktail. In contrast, when utilized as a reporter in nucleic acid amplification reactions, the loop region of an MB is complementary to a specific target DNA sequence [52]. For use as a molecular thermometer, the melting temperature T_m of the MB's stem region, which is determined by its length and GC content as well as by the ionic strength of the buffer [53, 54] must comply with the reaction temperature of the amplification technology of choice. For tHDA, the temperature range of interest is 60 to 65 °C and for PCR, 50 to 95 °C, respectively. Moreover, in order to interrogate proper temperature settings, the MB must ideally show a steep change in fluorescence around the melting point, which signals that the targeted temperature has been reached.

For our proof-of-concept study, in a first step, we designed four MBs with different lengths of the stem and loop sequences with calculated melting temperatures T_m of 47, 56, 64, and 70 °C in HDA buffer, respectively, to cover our application-relevant temperature range. These MBs, labeled with the fluorophore/quencher pairs 5′-ROX/3′-BHQ2 and 5′-ATTO 647N/3′-BHQ3, the sequences of which are shown in Table 2, were synthesized by standard methods and subsequently studied with respect to their melting behavior and their spectroscopic properties in PBS (Table 2). As follows from Table 2, length and GC content of the MB's stem sequence affect T_m of the two-dimensional stem-loop structure of the MBs. As shown in the ESM (see Table S1 comparing T_m data for PBS and HDA buffer and Fig. S10), the ionic strength of the buffer also slightly influences T_m.

As follows from the representative melting curves of MB-47, MB-56, MB-64, and MB-70 labeled with ROX (top panel) and ATTO 647N (lower panel) shown in Fig. 2, the T_m values obtained from the inflection points of the measured sigmoidal fluorescence intensity profiles, exploiting the strong increase in fluorescence intensity upon opening of the initially non-emissive MBs, are slightly higher than the calculated T_m values. Nevertheless, they display the expected control of T_m by the length of the stem sequence. For some MBs, especially for MB-70, the chosen fluorescent reporter-quencher pair seems to have a slight influence on T_m and the steepness of the melting curve. This effect has been described by other groups before, who observed a significant influence of the fluorophore/quencher moieties coupled to oligonucleotides on hybridization properties of the latter, i.e., a shift in the melting temperature [55].

Despite of this observation, with all MBs, a temperature resolution of about 0.5 °C could be achieved (see Figs. 2 and 3 and ESM, particularly Figs. S5 and S6 for representative uncertainties and Figs. S9 and S10 for PBS and HDA buffer) and all temperature-induced fluorescence changes were fully reversible as assessed by repeated temperature cycles (see ESM, Fig. S7). A similar behavior with slightly different T_m was observed in HDA buffer (see ESM, Figs. S8–S10 and Fig. S10 for a representative comparison of the influence of the buffer on the temperature profile of two

Table 2 MB sequences, melting temperatures (T_m) of stem sequences (*cal* calculated here for PBS; *exp* experimentally determined in PBS), experimentally determined temperature shift (ΔT_m), and the absorption ($\lambda_{abs,max}$) and emission ($\lambda_{em,max}$) maxima of the MBs in PBS

Sample	Sequence	$T_{m,calc}$ [°C]	$T_{m,exm}$ [°C]	$\Delta T_{m,exm}$ [°C]	$\lambda_{abs,max}$ [nm]	$\lambda_{em,max}$ [nm]
MB-47-ROX[a]	TACTC-TTTTTTTTTT-GAGTT	43.8	50.2 (±0.5)	44.0–59.0 (±0.6)	572	606
MB-56-ROX[a]	TCATGC-TTTTTTTTTT-GCATGT	53.6	59.1 (±0.2)	53.0–65.0 (±0.2)	573	608
MB-64-ROX[a]	TGCGTG-TTTTTTTTTT-CACGCT	61.4	64.1 (±0.2)	56.0–66.0 (±0.2)	577	601
MB-70-ROX[a]	TCGCATGG-TTTTTTTTTT-CCATGCGT	67.4	75.4 (±0.1)	70.0–80.0 (±0.2)	575	606
MB-47-ATTO 647N[b]	TACTC-TTTTTTTTTT-GAGTT	43.8	51.7 (±0.5)	47.0–59.0 (±0.5)	642	666
MB-56-ATTO 647N[b]	TCATGC-TTTTTTTTTT-GCATGT	53.6	59.9 (±0.2)	56.0–62.0 (±0.3)	641	666
MB-64-ATTO 647N[b]	TGCGTG-TTTTTTTTTT-CACGCT	61.4	70.2 (±0.3)	66.0–74.0 (±0.3)	642	665
MB-70-ATTO 647N[b]	TCGCATGG-TTTTTTTTTT-CCATGCGT	67.4	70.9 (±0.1)	65.0–77.0 (±0.1)	641	664

The ΔT_m values define the temperature interval of a MB where the temperature-dependent changes in fluorescence intensity are particularly large (see, e.g., Fig. 2 and Figs. S5 and S6 in the ESM) and where thus very small measurement uncertainties can be obtained. These values basically provide a measure for the range of operation for temperature sensing of a MB and correlate with its melting region. The relative standard deviations of $T_{m,cal}$ and ΔT_m are given in brackets

[a] Label (5′g 3′) 5′- ROX / BHQ2 -3′; lexc = 550 nm, solvent PBS

[b] Label (5′g 3′) 5′- ATTO 647N / BHQ3 -3′; lexc = 600 nm, solvent PBS

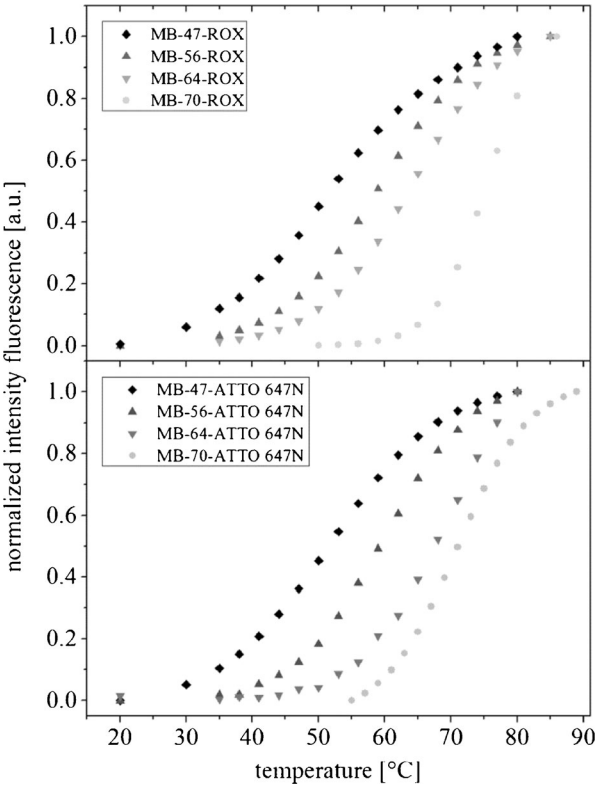

Fig. 2 Melting curves of four representative MBs labeled with ROX (*top*) and ATTO 647N (*bottom*) measured in PBS

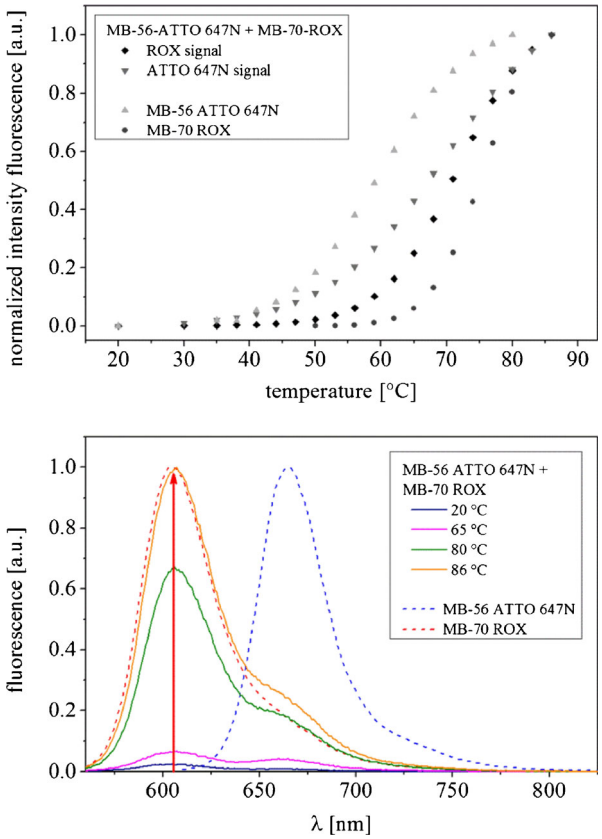

Fig. 3 *Top*: Normalized melting curves of a representative mixture of two MBs (MB-56-Atto 647N + MB-70-ROX; concentration ratio of 1:1) with different stem sequences labeled with different reporter-quencher pairs, read out using the fluorescence of ATTO 647N (*full black diamonds*) and ROX (*dark grey triangles*), respectively, in comparison to the corresponding single MBs (MB-56-Atto 647N: *light grey triangles*; MB-70-ROX: *full black circles*). *Bottom*: Temperature-dependent emission spectra of the MB mixture compared to the signals derived from MB-56 and MB-70, labeled with ROX and ATTO 647N, respectively, measured in PBS. The signal of the MB mixture was normalized to that of MB-56

representatively chosen MBs), thereby also underlining the stem sequence-specific influence of such matrix effects on the temperature or melting profile of MBs.

Temperature sensing with MB mixtures

In order to broaden the possibilities for temperature sensing, combinations of MBs with different stem sequences utilizing spectrally distinguishable pairs of fluorophore/quencher can be employed [35]. For example, advantageous for quality assurance of some diagnostic assays can be the use of two MBs with different T_m, labeled with a pair of temperature insensitive dyes like the reporters chosen by us that reveal spectrally distinguishable emission bands. This can be particularly interesting for temperatures below 45 °C where temperature measurements with MBs become less precise [35]. Moreover, the combination of MBs with different stem sequences can most likely improve the temperature resolution. This is exemplarily shown in Fig. 3 for a mixture of two MBs, here MB-56 and MB-70, differing in stem sequence, labeled with the spectrally distinguishable dyes ROX and ATTO 647N (Fig. 3, lower panel) and a quencher. Similar experiments with other MBs are provided in the ESM (Figs. S10–S12). As follows from Fig. 3 (top panel), the melting curve of the representative mixture of MB-56 and MB-70, recorded by measuring the ROX and ATTO 647N fluorescence at the respective emission maxima ($\lambda_{em,max}$(ROX) = 607 nm; $\lambda_{em,max}$(ATTO 647N) = 666 nm) lay between those derived from the single MBs. By using such a MB combination and a mathematical data evaluation, the temperature sensitivity can be increased, enabling a temperature resolution of 0.5 up to 0.1 °C. Moreover, such a MB combination can be used to set up an additional control for achieving or falling below a certain minimum temperature relevant for a specific diagnostic assay using "yes/no" decisions.

Temperature measurements in DNA-based assays with MBs

A simple method for isothermal amplification of nucleic acids increasingly employed for diagnostic DNA-based assays presents tHDA, which utilizes a helicase enzyme

to unspecifically unwind and separate double-stranded DNA (dsDNA) [5]. Subsequently, sequence-specific oligonucleotides hybridize to the single-stranded DNA signatures and are elongated by a strand-displacement DNA polymerase [5]. Finally, the newly synthesized double-stranded DNA section can be separated by the helicase again, which starts a new cycle of this exponential amplification scheme. The amplification process of tHDA reactions resembles the process of PCR, with the only exception that the unwinding activity of the DNA helicase replaces the heat denaturation for strand separation in PCR. The fact that this amplification method does not require complicated and power-hungry thermocycling equipment renders it ideal for POCT and assays performed with integrated microfluidic devices, such as the LabDisk Player by QIAGEN [56] or the sample-to-result molecular diagnostic system by Great Basin Scientific [57].

Hence, as proof-of-concept experiment that our temperature sensing MBs can be applied for monitoring isothermal nucleic acid amplification reactions, we chose tHDA and performed first proof-of-concept HDA experiments with the tHDA assay mixture and our MBs in the same reaction chamber using the real-time PCR instrument Rotor-Gene Q for assay readout, which is utilized by several thousand laboratories worldwide for performing, e.g., human molecular diagnostic assays. For this purpose, we added exemplarily MB-47 and MB-70 to a target-specific tHDA assay and measured the amplification-dependent fluorescence of the target-specific probe (Fig. 4, top panel) and the melting profiles of the MBs before and after tHDA reaction (Fig. 4, lower panel). In

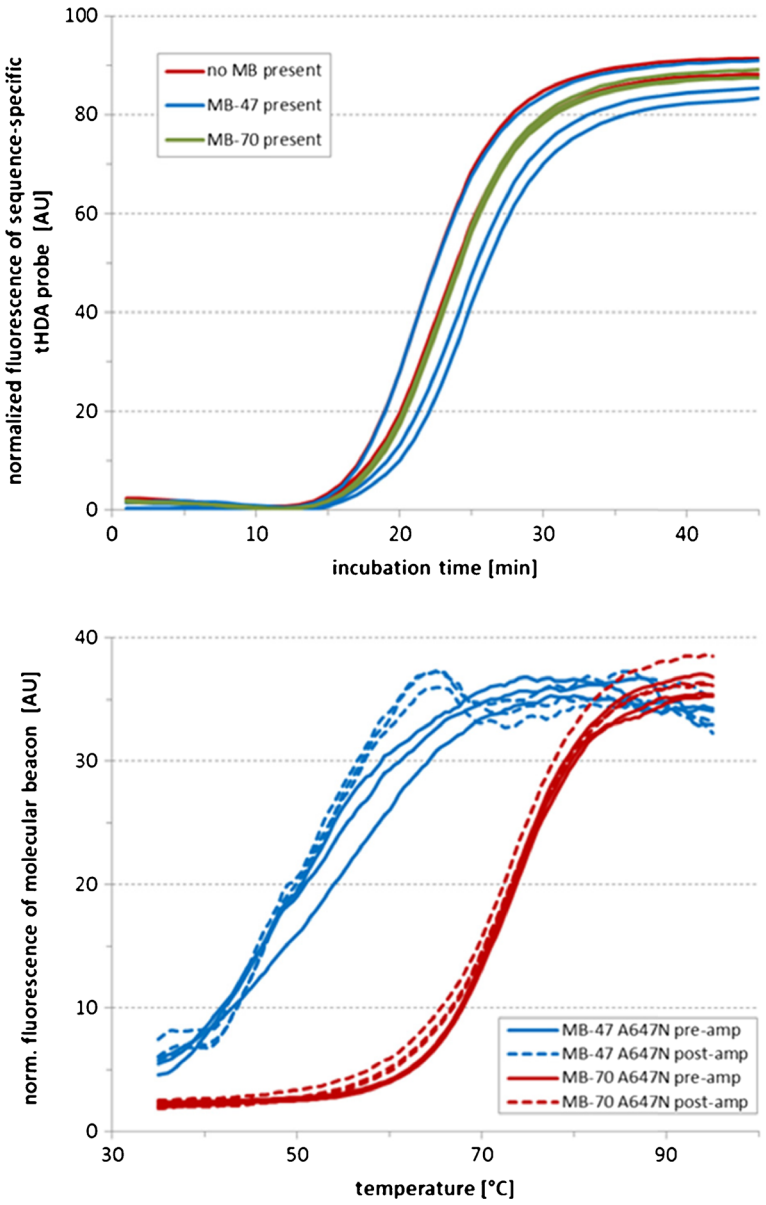

Fig. 4 *Top*: Fluorescence amplification profiles curves of a sequence-specific DNA probe during a representative tHDA reaction without (no MB; *red curve*) and in the presence of MB-47 (*blue curve*) or MB-70 (*green curve*) bearing the FRET pair ATTO 647N-BHQ3 (see Table 2). *Bottom*: Fluorescence intensity curves of two MBs (MB-47: *blue*; MB-70: *red*) applied to tHDA reaction mixtures containing a sequence-specific DNA probe labeled with a spectrally distinguishable fluorescent reporter, here Texas Red; *solid lines*: MB fluorescence in the presence of the tHDA reagents prior to the amplification reaction; *dotted lines*: MB fluorescence in the tHDA reaction mixture after amplification. The signal of the sequence-specific DNA probe, labeled with Texas Red, was detected at 610 nm, and the signals originating from MB-47 and MB-70 labeled with ATTO 647N were detected at 660 nm, respectively

molecular diagnostic applications, real-time fluorescence curves are typically analyzed close to the point, where fluorescence values rise above the background noise level and where the fluorescence increase is still exponential. Figure 4 (top) shows that the signals of the amplification probe show no significant deviations from the control reactions without MBs in this section of the fluorescence curve. This indicates that the amplification reaction is not inhibited by the MBs. Moreover, the isothermal amplification process did not alter the temperature-dependent melting profile of the MBs (Fig. 4, bottom) and the MBs kept their reversible temperature-dependent fluorescence behavior for many temperature cycles. This underlines that our MBs are very well suited for temperature signaling in assay mixtures. Although for the sake of simplicity, we performed the MB-based temperature measurements in conventional PCR reaction tubes, and other research groups have demonstrated that such results can be easily translated into an integrated microfluidic environment [58]; this is currently the focus of ongoing experiments.

Conclusion and outlook

Aiming at the development of a versatile platform of simple and very sensitive optical thermometers that can be directly integrated into a broad variety of DNA-based diagnostics assays for internal temperature monitoring and quality control, we developed a set of visible (vis) and red emissive molecular beacons (MBs) using dye-quencher pairs chosen based on temperature-dependent spectroscopic measurements in typical assay buffers. Spectroscopic studies of these MBs in buffers and representative MB-assay mixtures revealed that properly designed MBs can be employed for temperature measurements in molecular biological assays with a temperature resolution of less than 1 °C over a temperature range of 35–95 °C without interferences from assay components. Moreover, we could demonstrate the potential of spectrally distinguishable MB combinations to enable a broader temperature response range and to increase the temperature sensitivity to 0.5 °C or even 0.1 °C. This can be also beneficial for a stringent quality control of diagnostic assays.

Such fluorescent MB thermometers are thermally stable and compatible with different types of assay platforms and readout systems ranging from tube and microplate readers over microfluidic chips to PCR readout devices like thermal cyclers. Moreover, MBs enable a straightforward fine-tuning of their thermal and optical properties to meet assay-specific requirements. The vis and red emitting dyes ROX and ATTO 647N, used for MB design, can be combined with many other spectrally distinguishable, commercially available fluorescent reporters for the generation of the assay-specific signals like ATTO 647N, Cy5, and FAM (6-carboxyfluorescein) in the case of ROX and ROX as well as other rhodamine dyes or fluorescein derivatives like HEX (hexachloro-6-carboxy-fluorescein) in the case of ATTO 647N, respectively. For the use of combinations of a vis and a red MB for temperature sensing, assay readout can be performed with the blue excitation and detection channel, i.e., employing coumarin dyes such as Dylight 350 or Alexa Fluor 350 as labels. In this respect, we are currently accessing the potential of other shorter wavelength emitting fluorophores like rigid coumarins [50] for the design of a short wavelength absorbing and emitting blue MB, thereby complementing our versatile temperature sensor platform.

The use of MBs for temperature measurements and control, and thus for assay quality control, is particularly advantageous for reaction vessels that are part of a rotational microfluidic system or for chamber-less systems, utilizing, e.g., the electrowetting technology [42]. Such rotational systems, which apply a variety of forces on fluids within respective cartridges, are gaining in popularity [59, 60]. An advantage of these systems is that the fluid movement is controlled without valves and can be easily adapted to different needs just by changing the rotation protocol. Especially when it comes to running such instruments in resource-limited settings like developing countries [61], a tight internal control of reaction temperatures becomes a very important aspect of quality control for diagnostic procedures. This underlines the importance of our work for testing procedures in the molecular diagnostic space. Here, MBs are the only practical way to measure temperature with a maximum degree of freedom of fluid movement, because in this case, the temperature sensor is part of the reagent cocktail and thus carried with the fluid during assay performance. Moreover, for ready-to-use commercial assays using dried reagents, MBs are ideal as they can be freeze-dried like the assay components, which renders them superior particularly for this application to most other chemical systems suggested as temperature sensors.

Acknowledgments We gratefully acknowledge the contributions and help from Dr. W. Bremser for the statistical evaluation of the data, from M. Moser for the figures, and from Dr. D. Geissler for the calculation of the FRET efficiencies as well as the financial support from the Federal Ministry of Education and Research (BMBF; grant 16SV5439 from the project [RES]Check).

Compliance with ethical standards

Conflict of interest The authors declare that they have no conflict of interest.

References

1. Jaque D, Vetrone F. Luminescence nanothermometry. Nanoscale. 2012;4(15):4301–26. doi:10.1039/c2nr30764b.

2. Chin CD, Linder V, Sia SK. Commercialization of microfluidic point-of-care diagnostic devices. Lab Chip. 2012;12(12):2118–34. doi:10.1039/c2lc21204h.
3. (CLSI). CaLSI. Quantitative molecular methods for infectious diseases; approved guideline—second edition. CLSI document MM06-A2 (ISBN 1-56238-736-7) 2010;30(22).
4. Iwamoto T, Sonobe T, Hayashi K. Loop-mediated isothermal amplification for direct detection of Mycobacterium tuberculosis complex, M-avium, and M-intracellulare in sputum samples. J Clin Microbiol. 2003;41(6):2616–22. doi:10.1128/jcm.41.6.2616-2622.2003.
5. Vincent M, Xu Y, Kong HM. Helicase-dependent isothermal DNA amplification. EMBO Rep. 2004;5(8):795–800. doi:10.1038/sj.embor.7400200.
6. Jeong YJ, Park K, Kim DE. Isothermal DNA amplification in vitro: the helicase-dependent amplification system. Cell Mol Life Sci. 2009;66(20):3325–36. doi:10.1007/s00018-009-0094-3.
7. Mahony JB, Petrich A, Smieja M. Molecular diagnosis of respiratory virus infections. Crit Rev Clin Lab Sci. 2011;48(5–6):217–49. doi:10.3109/10408363.2011.640976.
8. Scheler O, Glynn B, Kurg A. Nucleic acid detection technologies and marker molecules in bacterial diagnostics. Expert Rev Mol Diagn. 2014;14(4):489–500. doi:10.1586/14737159.2014.908710.
9. Lahiri BB, Bagavathiappan S, Jayakumar T, Philip J. Medical applications of infrared thermography: a review. Infrared Phys Technol. 2012;55(4):221–35. doi:10.1016/j.infrared.2012.03.007.
10. Schäferling M. The art of fluorescence imaging with chemical sensors. Angew Chem Int Ed. 2012;51:2–25. doi:10.1002/anie.201105459.
11. Lou JF, Finegan TM, Mohsen P, Hatton TA, Laibinis PE. Fluorescence-based thermometry: principles and applications. Rev Anal Chem. 1999;18(4):235–84.
12. Ross D, Gaitan M, Locascio LE. Temperature measurements in microfluidic systems using a temperature-dependent fluorescent dye. Anal Chem. 2001;73(17):4117–23.
13. Ross D, Locascio LE. Fluorescence thermometry in microfluidics. CP684, temperature: its measurement and control in science and industry. American Institute of Physics; 2003.
14. Estrada-Perez CE, Hassan YA, Tan S. Experimental characterization of temperature sensitive dyes for laser induced fluorescence thermometry. Rev Sci Instrum. 2011;82(7):074901–7.
15. Freddi S, Sironi L, D'Antuono R, Morone D, Dona A, Cabrini E, et al. A molecular thermometer for nanoparticles for optical hyperthermia. Nano Lett. 2013;13(5):2004–10. doi:10.1021/nl400129v.
16. Homma M, Takei Y, Murata A, Inoue T, Takeoka S. A ratiometric fluorescent molecular probe for visualization of mitochondrial temperature in living cells. Chem Commun. 2015;51(28):6194–7. doi:10.1039/c4cc10349a.
17. Arai S, Suzuki M, Park SJ, Yoo JS, Wang L, Kang NY, et al. Mitochondria-targeted fluorescent thermometer monitors intracellular temperature gradient. Chem Commun. 2015;51(38):8044–7. doi:10.1039/c5cc01088h.
18. Nurmi J, Wikman T, Karp M, Lovgren T. High-performance real-time quantitative RT-PCR using lanthanide probes and a dual-temperature hybridization assay. Anal Chem. 2002;74(14):3525–32. doi:10.1021/ac020093y.
19. Brites CDS, Lima PP, Silva NJO, Millan A, Amaral VS, Palacio F, et al. Lanthanide-based luminescent molecular thermometers. New J Chem. 2011;35(6):1177–83. doi:10.1039/c0nj01010c.
20. Borisov SM, Mayr T, Klimant I. Poly(styrene-block-vinylpyrrolidone) beads as a versatile material for simple fabrication of optical nanosensors. Anal Chem. 2008;80(3):573–82. doi:10.1021/ac071374.
21. Takei Y, Arai S, Murata A, Takabayashi M, Oyama K, Ishiwata S, et al. A nanoparticle-based ratiometric and self-calibrated fluorescent thermometer for single living cells. ACS Nano. 2014;8(1):198–206. doi:10.1021/nn405456e.
22. Natrajan VK, Christensen KT. Two-color laser-induced fluorescent thermometry for microfluidic systems. Meas Sci Technol. 2009;20(1). doi:10.1088/0957-0233/20/1/015401.
23. Soleilhac A, Dagany X, Dugourd P, Girod M, Antoine R. Correlating droplet size with temperature changes in electrospray source by optical methods. Anal Chem. 2015;87(16):8210–7. doi:10.1021/acs.analchem.5600976.
24. Uchiyama S, Tsuji T, Ikado K, Yoshida A, Kawamoto K, Hayashi T, et al. A cationic fluorescent polymeric thermometer for the ratiometric sensing of intracellular temperature. Analyst. 2015;140(13):4498–506. doi:10.1039/c5an00420a.
25. Hu XL, Li Y, Liu T, Zhang GY, Liu SY. Intracellular cascade FRET for temperature imaging of living cells with polymeric ratiometric fluorescent thermometers. ACS Appl Mater Interfaces. 2015;7(28):15551–60. doi:10.1021/acsami.5b04025.
26. Gota C, Okabe K, Funatsu T, Harada Y, Uchiyama S. Hydrophilic fluorescent nanogel thermometer for intracellular thermometry. J Am Chem Soc. 2009;131(8):2766−+. doi:10.1021/ja807714j.
27. Liu J, Guo XD, Hu R, Xu J, Wang SQ, Li SY, et al. Intracellular fluorescent temperature probe based on triarylboron substituted poly N-isopropylacrylamide and energy transfer. Anal Chem. 2015;87(7):3694–8. doi:10.1021/acs.analchem.5b00887.
28. Shang L, Stockmar F, Azadfar N, Nienhaus GU. Intracellular thermometry by using fluorescent gold nanoclusters. Angew Chem Int Ed. 2013;52(42):11154–7. doi:10.1002/anie.201306366.
29. Sedlmeier A, Achatz DE, Fischer LH, Gorris HH, Wolfbeis OS. Photon upconverting nanoparticles for luminescent sensing of temperature. Nanoscale. 2012;4(22):7090–6. doi:10.1039/c2nr32314a.
30. Fischer LH, Harms GS, Wolfbeis OS. Upconverting nanoparticles for nanoscale thermometry. Angew Chem Int Ed. 2011;50(20):4546–51. doi:10.1002/anie.201006835.
31. Chen R, Ta VD, Xiao F, Zhang QY, Sun HD. Multicolor hybrid upconversion nanoparticles and their improved performance as luminescence temperature sensors due to energy transfer. Small. 2013;9(7):1052–7. doi:10.1002/smll.201202287.
32. Okabe K, Inada N, Gota C, Harada Y, Funatsu T, Uchiyama S. Intracellular temperature mapping with a fluorescent polymeric thermometer and fluorescence lifetime imaging microscopy. Nat Commun. 2012; 3. doi:10.1038/ncomms1714.
33. Tyagi S, Kramer FR. Molecular beacon probes that fluorescence upon hybridization. Nat Biotechnol. 1996;14(3):303–8.
34. Raphael MP, Christodoulides JA, Qadri SN, Qadri SA, Miller MM, Kurihara LK, et al. The use of DNA molecular beacons as nanoscale temperature probes for microchip-based biosensors. Biosens Bioelectron. 2008;24(4):888–92. doi:10.1016/j.bios.2008.07.028.
35. Ebrahimi S, Akhlaghi Y, Kompany-Zareh M, Rinnan A. Nucleic acid based fluorescent nanothermometers. ACS Nano. 2014;8(10):10372–82. doi:10.1021/nn5036944.
36. Ke GL, Wang CM, Ge Y, Zheng NF, Zhu Z, Yang CJ. L-DNA molecular beacon: a safe, stable, and accurate intracellular nanothermometer for temperature sensing in living cells. J Am Chem Soc. 2012;134(46):18908–11. doi:10.1021/ja3082439.
37. Barilero T, Le Saux T, Gosse C, Jullien L. Fluorescent thermometers for dual-emission-wavelength measurements: molecular engineering and application to thermal imaging in a microsystem. Anal Chem. 2009;81(19):7988–8000. doi:10.1021/ac901027f.
38. Nellaker C, Wallgren U, Karlsson H. Molecular beacon-based temperature control and automated analyses for improved resolution of melting temperature analysis using SYBR I Green chemistry. Clin Chem. 2007;53(1):98–103. doi:10.1373/clinchem.2006.075184.
39. Tyagi S, Marras SAE, Kramer FR. Wavelength-shifting molecular beacons. Nat Biotechnol. 2000;18(11):1191–6.

40. Stellacci FCAB, Meyer-Friedrichsen T, Wenseleers W, Marder SR, Perry JW. Ultrabright supramolecular beacons based on the self-assembly of two-photon chromophores on metal nanoparticles. J Am Chem Soc. 2003;125(2):328–9.
41. Roh SS, Smith LE, Lee JS, Via LE, Barry CE, Alland D et al. Comparative evaluation of sloppy molecular beacon and dual-labeled probe melting temperature assays to identify mutations in mycobacterium tuberculosis resulting in rifampin, fluoroquinolone and aminoglycoside resistance. Plos One. 2015;10(5). doi:10.1371/journal.pone.0126257.
42. Fair RB, Khlystov A, Tailor TD, Ivanov V, Evans RD, Griffin PB, et al. Chemical and biological applications of digital-microfluidic devices. IEEE Des Test Comput. 2007;24(1):10–24. doi:10.1109/mdt.2007.8.
43. Würth C, Grabolle M, Pauli J, Spieles M, Resch-Genger U. Relative and absolute determination of fluorescence quantum yields of transparent samples. Nat Protoc. 2013;8(8):1535–50. doi:10.1038/nprot.2013.087.
44. Wurth C, Lochmann C, Spieles M, Pauli J, Hoffmann K, Schuttrigkeit T, et al. Evaluation of a commercial integrating sphere setup for the determination of absolute photoluminescence quantum yields of dilute dye solutions. Appl Spectrosc. 2010;64(7):733–41.
45. Markham NR, Zuker M. DINAMelt web server for nucleic acid melting prediction. Nucleic Acids Res. 2005;33:W577–81. doi:10.1093/nar/gki591.
46. Resch-Genger U, DeRose PC. Characterization of photoluminescence measuring systems (IUPAC Technical Report). Pure Appl Chem. 2012;84(8):1815–35.
47. Lakowicz JR. Principles of fluorescence spectroscopy. 3rd ed. Principles of fluorescence spectroscopy. New York: Springer Science + Business Media, LLC; 2006.
48. Moreira BG, You Y, Behlke MA, Owczarzy R. Effects of fluorescent dyes, quenchers, and dangling ends on DNA duplex stability. Biochem Biophys Res Commun. 2005;327(2):473–84. doi:10.1016/j.bbrc.2004.12.035.
49. Kubin RF, Fletcher AN. Fluorescence quantum yields of some rhodamine dyes. J Lumin. 1982;27:455–62.
50. Mao DQ, Liu XG, Qiao QL, Yin WT, Zhao M, Cole JM, et al. Coumarin 545: an emission reference dye with a record-low temperature coefficient for ratiometric fluorescence based temperature measurements. Analyst. 2015;140(4):1008–13. doi:10.1039/c4an02075h.
51. Fare TL, Coffey EM, Dai H, He YD, Kessler DA, Kilian KA, et al. Effects of atmospheric ozone on microarray data quality. Anal Chem. 2003;75(17):4672–5.
52. Piatek AS, Tyagi S, Pol AC, Telenti A, Miller LP, Kramer FR, et al. Molecular beacon sequence analysis for detecting drug resistance in Mycobacterium tuberculosis. Nat Biotechnol. 1998;16(4):359–63. doi:10.1038/nbt0498-359.
53. Bonnet G, Krichevsky O, Libchaber A. Kinetics of conformational fluctuations in DNA hairpin-loops. Proc Natl Acad Sci U S A. 1998;95(15):8602–6. doi:10.1073/pnas.95.15.8602.
54. Goddard NL, Bonnet G, Krichevsky O, Libchaber A. Sequence dependent rigidity of single stranded DNA. Phys Rev Lett. 2000;85(11):2400–3. doi:10.1103/PhysRevLett.85.2400.
55. You Y, Tataurov AV, Owczarzy R. Measuring thermodynamic details of DNA hybridization using fluorescence. Biopolymers. 2011;95(7):472–86. doi:10.1002/bip.21615.
56. Lutz S, Weber P, Focke M, Faltin B, Hoffmann J, Muller C, et al. Microfluidic lab-on-a-foil for nucleic acid analysis based on isothermal recombinase polymerase amplification (RPA). Lab Chip. 2010;10(7):887–93. doi:10.1039/b921140c.
57. Hicke B, Pasko C, Groves B, Ager E, Corpuz M, Frech G, et al. Automated detection of toxigenic clostridium difficile in clinical samples: isothermal tcdB amplification coupled to array-based detection. J Clin Microbiol. 2012;50(8):2681–7. doi:10.1128/jcm.00621-12.
58. Keller M, Naue J, Zengerle R, von Stetten F, Schmidt U. Automated forensic animal family identification by nested PCR and melt curve analysis on an off-the-shelf thermocycler augmented with a centrifugal microfluidic disk segment. Plos One. 2015;10(7). doi:10.1371/journal.pone.0131845.
59. Czilwik G, Messinger T, Strohmeier O, Wadle S, von Stetten F, Paust N, et al. Rapid and fully automated bacterial pathogen detection on a centrifugal-microfluidic LabDisk using highly sensitive nested PCR with integrated sample preparation. Lab Chip. 2015;15(18):3749–59. doi:10.1039/c5lc00591d.
60. Stumpf F, Schwemmer F, Hutzenlaub T, Baumann D, Strohmeier O, Dingemanns G, et al. LabDisk with complete reagent prestorage for sample-to-answer nucleic acid based detection of respiratory pathogens verified with influenza A H3N2 virus. Lab Chip. 2016;16(1):199–207. doi:10.1039/c5lc00871a.
61. Escadafal C, Faye O, Sall AA, Faye O, Weidmann M, Strohmeier O et al. Rapid molecular assays for the detection of yellow fever virus in low-resource settings. PLoS Negl Trop Dis. 2014;8(3). doi:10.1371/journal.pntd.0002730.